EurJIC European Journal of Inorganic Chemistry

ChemPubSoc Europe

FULL PAPER

DOI:10.1002/ejic.201500656

Comparative Study of the Catalytic Amination of Benzylic C–H Bonds Promoted by Ru(TPP)$(py)_2$ and Ru(TPP)(CO)

Gabriele Manca,*[a] Carlo Mealli,[a] Daniela Maria Carminati,[b] Daniela Intrieri,[b] and Emma Gallo*[b]

Keywords: Ruthenium / Porphyrinoids / Amination / Density functional calculations / Reaction mechanisms

A combined experimental and DFT-based theoretical analysis elucidated the influence of the axial ligand L on the catalytic activity of Ru(porphyrin)L complexes in promoting the amination of benzylic C–H bonds by organic azides (RN_3). Experimental data indicated that the catalytic activity of Ru(TPP)(CO) (**1**) (TPP = dianion of tetraphenylporphyrin) is comparable to that of Ru(TPP)$(py)_2$ (**2**) (py = pyridine). DFT modelling disclosed that **2** can be regarded as a precatalyst that becomes active after the endergonic loss of one pyridine ligand to give the unsaturated species [Ru](py) (**11**) {[Ru] = Ru(porphine)}. This complex would react with RN_3 to give the mono-imido singlet complex [Ru](py)$(NR)_S$ ($\mathbf{6_S}$), which can be easily transformed into the triplet isomer $\mathbf{6_T}$ having diradical character at the imido N atom. The subsequent formation of the benzylic amine $PhCH_2NHR$ occurs through a radical homolytic activation of one C–H bond of the toluene substrate ($PhCH_3$). Conversely, by staying on the singlet potential-energy surface, $\mathbf{6_S}$ can undergo dissociation of the pyridine ligand to form [Ru](NR). This complex can activate another RN_3 molecule to form the bis-imido compound $[Ru](NR)_2$, which is also catalytically active. At this point, the mechanism becomes independent of the nature of the original ligand L coordinated to [Ru].

Introduction

The catalytic syntheses of nitrogen-containing compounds are important for their potential use as precursors of biological and pharmaceutical compounds.[1,2] In response to the demand for sustainable chemistry, the employment of organic azides (RN_3) as nitrogen sources for the synthesis of aza compounds[3–10] is constantly growing. In fact, this class of aminating reagents shows high ecocompatibility due to the formation of the benign molecular nitrogen as the only by-product of the nitrene ("RN") transfer reaction to an organic molecule. Among available organic azides, the aryl azides are very interesting nitrogen sources because of their convenient reactivity/stability relationship and their easy syntheses from the corresponding amines. More extensive employment of these aminating agents is also favoured by their commercial availability, thanks to an efficient and safe procedure to obtain aryl azides in bulk amounts.[11]

Metal porphyrin complexes efficiently promote amination reactions of saturated and unsaturated hydrocarbons by aryl azides,[12–29] and they show very good activity in the amination of activated sp^3 C–H bonds. Ruthenium(II) porphyrins[19,21,30] are active catalysts in the synthesis of allylic and benzylic amines. They are also efficient in the amination of benzylic C–H bonds in the α or β positions with respect to an ester group to yield the corresponding and biologically relevant α- and β-amino esters.[23,31–33]

One of the most extensively used amination catalyst is the five-coordinate complex Ru(TPP)(CO) (**1**) (TPP = dianion of tetraphenylporphyrin), which has the π-acceptor CO ligand in the axial position. The vacant coordination site in the *trans* position is suitable for azide activation. Kinetic[20] and DFT[27] studies indicated that the reaction of Ru(TPP)CO with ArN_3 first affords the octahedral mono-imido complex Ru(TPP)(NAr)(CO) in a singlet state, which can be transformed into a slightly more stable triplet with the two unpaired spins largely localised at the NAr ligand. Such a diradical can promote the activation of different organic substrates,[27] in particular the homolysis of a C–H bond of a hydrocarbon with consequent formation of the corresponding amine[27a] by the so-called rebound mechanism.[34] Conversely, if the species Ru(TPP)(NAr)(CO) remains a singlet, the bis-imido complex Ru(TPP)$(NAr)_2$ (**7**)[18,20] is formed through CO departure and another azide activation. Complex **7** can also behave as a diradical species for a similar type of amination chemistry.

[a] Istituto di Chimica dei Composti OrganoMetallici, ICCOM-CNR,
Via Madonna del Piano 10, 50019 Sesto Fiorentino, Italy
E-mail: gabriele.manca@iccom.cnr.it
www.iccom.cnr.it
[b] Department of Chemistry, University of Milan,
Via Golgi 19, 20133 Milan, Italy
E-mail: emma.gallo@unimi.it
www.unimi.it

Supporting information for this article is available on the WWW under http://dx.doi.org/10.1002/ejic.201500656.

Both CO and NR ligands, placed *trans* to the vacant coordination site at which the azide is activated, combine π-acceptor and σ-donor abilities. To analyse the catalytic influence of the electronic features of the axial ligand, we here report the combined experimental and computational study of the catalytic behaviour of Ru(TPP)(py)$_2$ (**2**). Although the physicochemical properties of **2** were already elucidated by a variety of experimental methods, such as electrochemistry,[35,36] UV/Vis absorption, emission, resonance Raman[37–41] and picosecond transient absorption,[42,43] the use of this complex to catalyse C–H amination by organic azides has not yet been reported.

Results and Discussion

Experimental Studies on the Catalytic Activity of Ru(TPP)(py)$_2$ (2)

The bis-pyridine Ru^{II} complex **2** was prepared in accordance with a reported synthetic procedure[40] and used to catalyse the reaction between aryl azides (ArN$_3$) and various benzylic substrates of general formula R′R′′R′′′C–H to yield the corresponding aminated compounds **3a**–**3h** (Table 1). 3,5-Bis(trifluoromethyl)phenyl azide was used as the aminating agent, with the sole exception of the synthesis of compound **3c**, for which 4-*tert*-butyl azide was employed.

Data reported in Table 1 indicate that complex **2** is a good catalyst of C–H amination, and its catalytic efficiency is comparable to that of Ru(TPP)CO (**1**) when used to catalyse the synthesis of the same compounds.[19,33] As observed in **1**-catalysed reactions, **2** was more effective in activating electron-deficient azides. Indeed, the reaction of 4-*tert*-butyl azide with ethylbenzene yielded **3c** in a low yield (Table 1, entry 2), which suggested an electrophilic role of azide in the amination reaction. Complex **2** was also active in promoting the amination of the allylic C–H bond of cyclohexene by 3,5-bis(trifluoromethyl)phenyl azide. The corresponding allylic amine *N*-(cyclohex-2-en-1-yl)-3,5-bis(trifluoromethyl)aniline (**3i**)[20] was formed in 0.75 h with 77% yield. For all the described reactions, NMR and GC-MS analyses of the crude product revealed the formation of ArN=NAr and ArNH$_2$ side products derived from partial decomposition of the employed azide.

Considering that in previous reactions catalysed by Ru(TPP)CO (**1**),[19,33] slightly different experimental conditions were used, the synthesis of compound **3f** was repeated in the presence of complex **1** by using the experimental conditions described in Table 1 to give 90% of the benzylic amine in 1 h. Even though the yield was higher than that obtained in the presence of **2** (Table 1, entry 5), the reaction time increased from 20 min to 1 h. An attempt was made to enhance the selectivity of **3f** by reducing the formation of side products. Thus, azide was slowly added to the reaction mixture with a syringe pump over 1.5 h, but unfortunately the reaction yield did not increase. Although the reaction yield was enhanced to 72% by working at 70 °C, the time required for full conversion of the azide to **3f** became excessively long (7.0 h). Clearly, the lower working temperature inhibited the formation of side products as well as the activation of the azide, which was more effective at the refluxing temperature of cumene (≈ 150 °C).

Table 1. Synthesis of compounds **3a**–**3h** catalysed by **2**.[a]

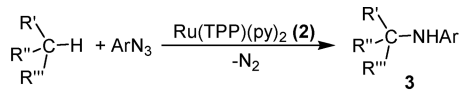

Entry	Product	Ar	*t* (h)[b]	3	Yield %[c]
1	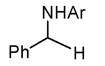	3,5-(CF$_3$)$_2$C$_6$H$_3$	0.5 (1)[d]	**3a**	62 (66)[d]
2	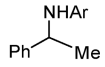	3,5-(CF$_3$)$_2$C$_6$H$_3$ 4-*t*BuC$_6$H$_4$	0.6 (4)[d] 0.5	**3b** **3c**	85 (85)[d] 32
3	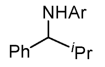	3,5-(CF$_3$)$_2$C$_6$H$_3$	0.5 (1)[d]	**3d**	50 (75)[d]
4[e]	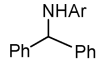	3,5-(CF$_3$)$_2$C$_6$H$_3$	0.3 (0.4)[d]	**3e**	65 (65)[d]
5	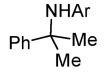	3,5-(CF$_3$)$_2$C$_6$H$_3$	0.25 (1.15)[d]	**3f**	61 (90)[d]
6[f]	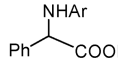	3,5-(CF$_3$)$_2$C$_6$H$_3$	12 (6)[g]	**3g**	56 (80)[g]
7[f]	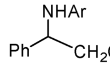	3,5-(CF$_3$)$_2$C$_6$H$_2$	8 (10)[g] 1.3	**3h**	55 (77)[g] 82[h]

[a] Experimental conditions: 6.8×10^{-3} mmol of the catalyst (2% with respect to ArN$_3$) in 15.0 mL of refluxing hydrocarbon substrate as the reaction solvent. [b] Time required for complete azide conversion, determined by IR spectroscopic monitoring of the decrease in N$_3$ absorbance at about 2115 cm^{-1}. [c] Yields based on ArN$_3$ and determined by ^{1}H NMR spectroscopy (2,4-dinitrotoluene as the internal standard). [d] Reaction catalysed by **1**.[19] [e] Reaction run at 150 °C. [f] Reaction run at 80 °C. [g] Reaction catalysed by **1**.[33] [h] 6% of **2** was used.

Considering the biological relevance of β-amino esters, the synthesis of 3-[3,5-bis(trifluoromethyl)phenylamino]-3-phenylpropanoate (**3h**) was studied under different experimental conditions. As reported in entry 7 of Table 1, the best yield of the desired compound **3h** (82%) was obtained by using a catalytic ratio **2**/3,5-bis(trifluoromethyl)phenyl azide of 1:15 in methyl hydrocinnamate as the reaction solvent.

The reaction was also performed in refluxing benzene with a catalytic ratio **2**/azide/hydrocarbon of 1:15:1000, but compound **3h** was formed in 5 h with 60% yield. Importantly, the reaction catalysed by **2** is faster than that performed in the presence of Ru(TPP)CO (**1**), for which 77% yield was obtained after 10 h with a catalytic ratio **1**/azide/hydrocarbon of 1:15:1000 in refluxing benzene. This last result is important because it indicates that two coaxial pyridine ligands do not hamper the efficiency of the catalyst, even though the latter must vacate one coordination site to allow the activation of the azide and the subsequent amin-

ation reaction (see the conclusions of the theoretical analysis below). The reaction time was halved by increasing the methyl hydrocinnamate concentration, and 70% yield of **3h** was obtained in 2.5 h by employing a catalytic ratio **2**/azide/hydrocarbon of 1:15:2500. Data reported above indicate the importance of using high methyl hydrocinnamate concentrations to achieve good catalytic performance. To reduce the reaction costs, the excess hydrocarbon was recovered at the end of the reaction by a simple distillation process, as already reported by us for the same reaction catalysed by complex **1**.[33]

To obtain experimental information on the strength of the Ru–py bond in **2**, we studied the process of pyridine substitution by dimethyl sulfoxide (DMSO). The reaction with DMSO quantitatively yielded the complex $Ru(TPP)(DMSO)_2$ (**4**), which supports the hypothesis that the two pyridine ligands in **2** are not irreversibly coordinated to the metal centre and can be displaced by another 2e-donor ligand (Scheme 1, path a). In view of this result, we treated **2** with an equimolar amount of ArN_3 in order to substitute pyridine by an azide ligand to give Ru^{II}-(TPP)(py)(ArN_3) (**5**) or Ru^{IV}(TPP)(py)(NAr) (**6**), which is derived from **5** by elimination of molecular nitrogen (Scheme 1, path b). Unfortunately, we did not observe the coordination of one ArN_3 ligand to the metal centre yielding **5** or the mono-imido derivative **6**. The NMR analysis of the crude reaction product revealed the presence of an equimolar mixture of $Ru(TPP)(py)_2$ (**2**) and bis-imido complex $Ru(TPP)(NAr)_2$ (**7**). This suggests that, even if compounds **5** and **6** are momentarily formed, they are too elusive to be experimentally detected, most likely because **7** is quickly formed as the thermodynamically stable product (Scheme 1, path c). Then, we tried to detect the formation of the key intermediate Ru^{IV}(TPP)(py)(NAr) (**6**) in the reaction of equimolar amounts of **2** and **7**. Unfortunately, the desired nitrene-transfer reaction from **7** to **2** did not occur, and the formation of the elusive mono-imido intermediate **6** was not observed (Scheme 1, path d).[20,27]

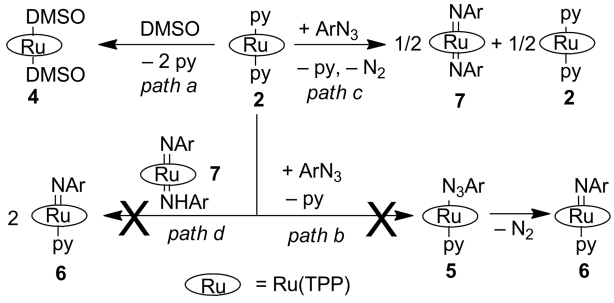

Scheme 1. The reactivity of complex **2** towards DMSO, ArN_3 and complex **7**.

In conclusion, all the collected experimental data indicate that the catalytic activity of the bis-pyridine complex **2** in the amination of C–H bonds by aromatic azides is comparable to, and in some cases better than, that of Ru(TPP)CO (**1**). This result is somewhat surprising, because **2** first needs to vacate one coordination site for azide activation. Moreover, the pyridine ligand differs from CO in having no significant π-acceptor capability, which was computationally found to be important in singlet/triplet intersystem crossing for promotion of the radical activity. For these reasons, we compare in the following theoretical section some important electronic aspects of catalysts **1** and **2** as well as the corresponding reaction profiles of amination reactions.

Computational Studies

General Aspects of the Amination Reaction Catalysed by [Ru](CO) (1)

Our previous computational studies illustrated the possible mechanisms of the catalytic allylic amination of cyclohexene by an RN_3 molecule.[27] With [Ru](CO) (**1**) {[Ru] = Ru(porphine), porphine = parent compound of porphyrins} as catalyst, the overall process consists of the two interconnected cycles (a) and (b) shown in Scheme 2. The mechanistic proposal is supported by kinetic investigations and by the isolation and characterisation of the bis-imido complex $Ru(TPP)(NR)_2$ (**7**) {R = 3,5-bis(trifluoromethyl)phenyl}, which is catalytically active in several hydrocarbon aminations.[18,20]

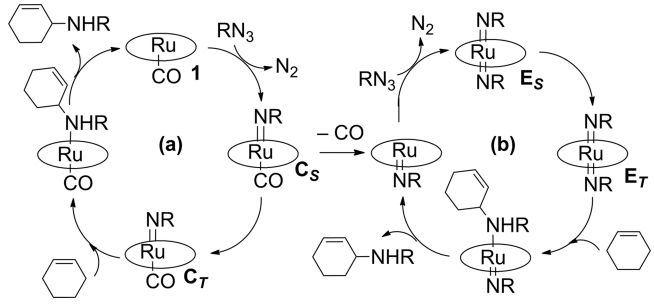

Scheme 2. Overall mechanism of the **1**-catalysed C–H amination of cyclohexene by an organic azide (RN_3).

Cycle (a) starts with RN_3 activation by complex **1** to give the mono-imido species $[Ru](CO)(NR)_S$ ($\mathbf{C_S}$) via a well-defined TS (not shown in Scheme 2).[27] Importantly, the employment of CH_3N_3 in place of the experimentally used 3,5-bis(trifluoromethyl)phenyl azide does not change the overall reaction profile. Only the barrier of +26.8 kcal mol^{-1} is about 25% higher than that optimised by modelling the experimentally used azide. Since such a difference is not dramatic, CH_3N_3 is indicated as RN_3 in all the subsequent modelling, including that relative to reactions promoted by **2** (see below).

In cycle (a) the singlet minimum $\mathbf{C_S}$ is first obtained after the TS, although its triplet isomer $[Ru](CO)(NR)_T$ ($\mathbf{C_T}$) is –3.7 kcal mol^{-1} more stable. The implied intersystem crossing is fundamental to trigger radical reactivity, given that the two unpaired electrons are largely localised at the axial imido N atom. Complex $\mathbf{C_T}$ is able to promote the homolytic cleavage of a C–H bond of cyclohexene (C_6H_{10}) to form the mono-amido $[Ru](CO)(NHR)_D$ doublet interme-

diate together with the free cyclohexenyl radical ($C_6H_9^{\cdot}$). Subsequently, the two radicals pair their spins to afford the desired allylic amine $(C_6H_9)NHR$, first as a ligand and then as a free molecule. This process corresponds to the known rebound mechanism.[34] The overall estimated free-energy gain for cycle (a) is –44.8 kcal mol^{-1}.[27]

If not promptly converted to $\mathbf{C_T}$, $\mathbf{C_S}$ has the alternative possibility of losing the CO apical ligand to afford access to cycle (b) of Scheme 2. The derived five-coordinate [Ru](NR) species has a vacant coordination site to activate a second azide molecule, which, after another similar TS, affords the bis-imido complex $[Ru](NR)_2$ ($\mathbf{E_S}$). In principle, the latter singlet complex also has the possibility of transforming into the triplet isomer $\mathbf{E_T}$, although such process is endergonic rather than exergonic like the $\mathbf{C_S}\rightarrow\mathbf{C_T}$ transformation.

Then, one of the two coordinated NR groups of $\mathbf{E_T}$ may initiate radical reactivity towards the cyclohexene substrate. Hence, a similar rebound mechanism leading to the same allylic amine product with an energy balance comparable with that of cycle (a) is also possible in this case.

Comparison of the Amination of Toluene and Cyclohexene Catalysed by [Ru](CO) (1)

The mechanism of Scheme 2 refers to the **1**-catalysed allylic amination of cyclohexene, whereas the catalytic activity of **2** was mainly studied in the amination of the benzylic substrates indicated in Table 1. Since the behaviour of **1** was previously highlighted only toward allylic amination,[27] we now briefly illustrate some comparative aspects of benzylic amination promoted by the same catalyst **1**.[19,20] Toluene ($PhCH_3$) was therefore modelled as the benzylic substrate, and Scheme 3 shows the energy profile relative to the activation of the methylic C–H bond by the diradical [Ru](CO)$(NR)_T$ ($\mathbf{C_T}$) complex. As discussed above, $\mathbf{C_T}$ is formed

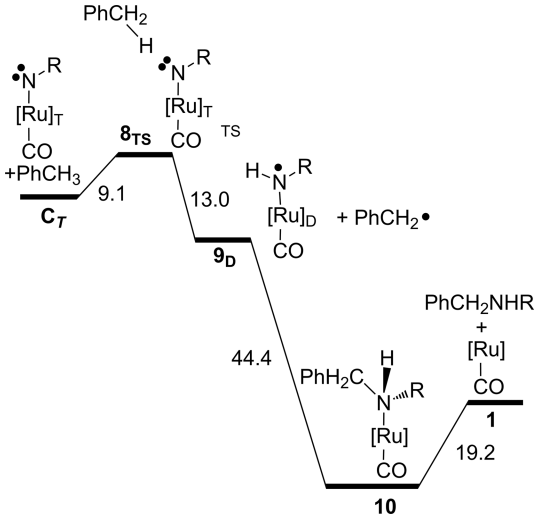

Scheme 3. Energy profile for formation of the benzylic amine $PhCH_2NHR$ starting from the mono-imido diradical [Ru](CO)(NR) ($\mathbf{C_T}$).

independent of the chemical nature of the hydrocarbon substrate (cyclohexene or toluene).

The energy barrier at the transition state (TS) {[Ru](CO)$(NR)_T$*$PhCH_3$}$_{TS}$ ($\mathbf{8_{TS}}$, see Figure S1) is only slightly higher than that obtained with cyclohexene (+9.1 vs. +7.5 kcal mol^{-1}). Additionally, the following step toward the combined doublet [Ru](CO)$(NHR)_D$ ($\mathbf{9_D}$) and the free tolyl radical $PhCH_2^{\cdot}$ is somewhat less exergonic (–13.0 vs. –18.3 kcal mol^{-1}), which suggests a possibly more difficult process. On the other hand, the recombination of the two radicals to give the diamagnetic amino complex [Ru](CO){HN(R)CH_2Ph} (**10**) is more exergonic than that in the corresponding allylic amination (–44.4 vs. –38.6 kcal mol^{-1}). The final separation of the benzylic amine ($PhCH_2NHR$) from the metal is somewhat more hindered than that of the allylic amine $(C_6H_9)NHR$ (+19.2 vs. +12.9 kcal mol^{-1}). Such an important difference is reflected in the overall lower exergonicity of the amination process involving toluene compared to that involving cyclohexene (–37.2 vs. –44.8 kcal mol^{-1}, respectively).

Catalytic Activity of [Ru](py)$_2$ (2)

Benzylic amination catalysed by [Ru](py)$_2$ (**2**) was computationally analysed. The isolated octahedral precursor **2** was optimised (Figure S2) with two identical Ru–N_{py} distances of 2.09 Å, which fully match those of the available X-ray structure.[44,45] To behave as a catalyst, **2** must first lose one pyridine ligand to allow activation of the azide, similar to what happens at **1**. The optimised five-coordinate complex [Ru](py) (**11**) (Figure 1, a) has an about 0.1 Å shorter Ru–N_{py} bond with respect to that of [Ru](py)$_2$ (**2**). This is attributable to the loss of any *trans* influence on vacating one of the two coordination sites. The transformation of **2** into **11** involves a high energy cost of +22.1 kcal mol^{-1} (first step in Scheme 4). All attempts to identify a TS for the dissociation failed, while a scanning technique indicated that the process proceeds monotonously uphill. Therefore, the formation of **11**, corroborated by its subsequent catalytic activity, must be attributed to the relatively high temperature used in the catalytic experiments (> 70 °C, see Table 1).

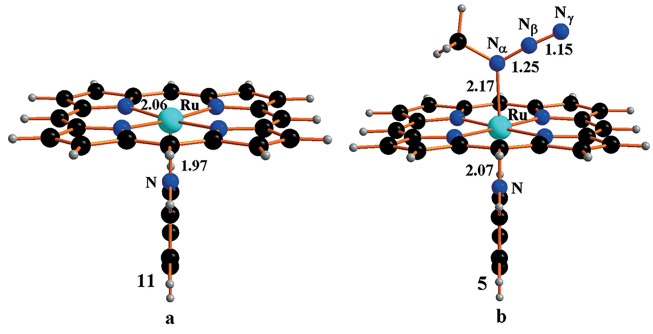

Figure 1. Optimised structures of (a) [Ru](py) (**11**) and (b) [Ru](py)(RN_3) (**5**).

The vacant coordination site at **11** allows the coordination of one azide to the metal to give the adduct [Ru](py)-

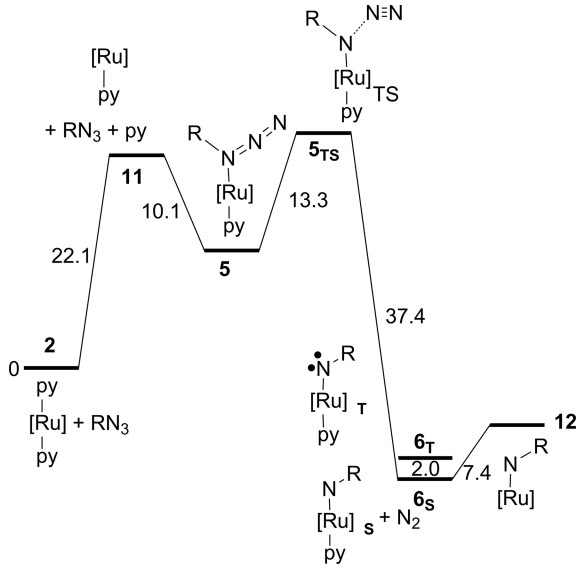

Scheme 4. Energy profile for formation of mono-imido complex [Ru](NR) (**12**) starting from [Ru](py)$_2$ (**2**).

(RN_3) (**5**) of Figure 1 (b). Note that **5** has a higher stabilisation energy than the corresponding carbonylated complex [Ru](CO)(RN_3): –10.1 versus –3.5 kcal mol^{-1}. In this respect, we recall that **1** is largely stable as an unsaturated species, whereas its azide adduct [Ru](CO)(RN_3) is stabilised only by weak dispersion forces,[27] as clearly established by usage of the DFTD functional.[46]

The greater stabilisation of [Ru](py)(RN_3) (**5**) is reflected in the shorter Ru–N_{azide} coordination bond compared to that in [Ru](CO)(RN_3) (2.17 vs. 2.31 Å) due to the stronger CO *trans* influence. The significant energy gain of the adduct **5** may in part compensate the energy previously lost with the first pyridine departure from **2**, and thus justifies the observed catalytic activity of Ru(TPP)(py)$_2$.

Azide activation by **11** proceeds, as described before, through the TS $\mathbf{5_{TS}}$ (Figure 2), which shows previously observed structural features.[27] At this point, diatomic N_2 is about to be released, since the N_β–N_γ distance is short as 1.14 Å, while its separation from the still-coordinated N_α atom is already quite large (1.58 Å). In the process, the N_3

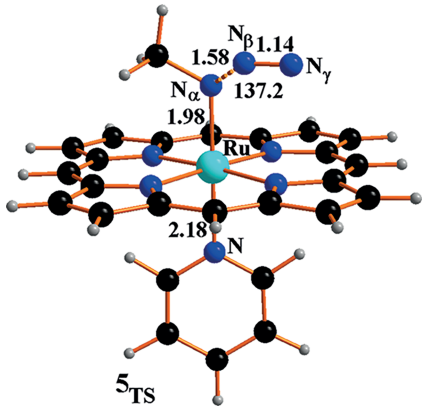

Figure 2. Optimised structure of [Ru](py)(RN_3)$_{TS}$ ($\mathbf{5_{TS}}$).

group has already lost its original linearity, since the angle N_α–N_β–N_γ is 137.2°.

In Scheme 4, the barrier at $\mathbf{5_{TS}}$ of +13.3 kcal mol^{-1} is about 50% lower than that in the corresponding process catalysed by **1** (+26.8 kcal mol^{-1}). Therefore, after the initially difficult activation of the catalytic reactivity, the evolution of the amination reaction seems to be facilitated by the presence of pyridine. Not only is the barrier lower, but also the following imido product [Ru](py)(NR)$_S$ ($\mathbf{6_S}$ in Figure 3, a) is significantly more stable than the carbonylated analogue [Ru](CO)(NR)$_S$ ($\mathbf{C_S}$) (–37.4 vs. –27.9 kcal mol^{-1}).

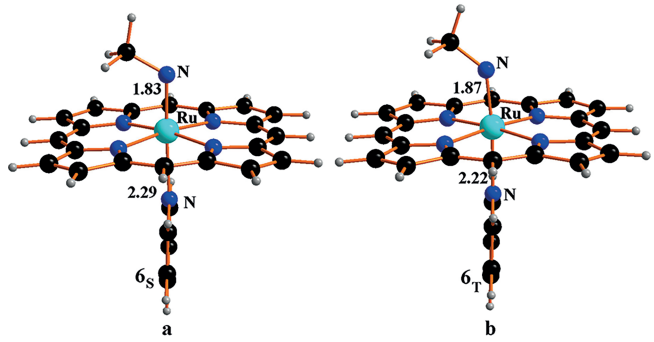

Figure 3. Optimised structure of the spin isomers (a) [Ru](py)(NR)$_S$ ($\mathbf{6_S}$) and (b) [Ru](py)(NR)$_T$ ($\mathbf{6_T}$).

Importantly, the complex $\mathbf{6_S}$, analogously to $\mathbf{C_S}$, is found to undergo intersystem crossing to the triplet spin isomer $\mathbf{6_T}$ (Figure 3, b), which is the fundamental step for promoting the radical reactivity. The main difference between the two pairs of spin isomers is that, while the $\mathbf{C_S}$→$\mathbf{C_T}$ interconversion is somewhat exergonic, the $\mathbf{6_S}$→$\mathbf{6_T}$ process is endergonic (–3.7 vs. +2.0 kcal mol^{-1}), but in any case the differences are not large enough to hamper the following radical reactivity.

For [Ru](CO)(NR)$_S$ ($\mathbf{C_T}$), an orbital analysis suggested that two singly populated MO levels of the $\mathbf{C_T}$ triplet receive a favourable contribution from the two CO π* orbitals.[27] In fact, a percentage of the latter is present in the singly occupied molecular orbitals (SOMOs), which are mainly combinations of metal d_π (d_{xz}, d_{yz}) and NR p_π orbitals. This is not exactly the case for $\mathbf{6_T}$, in which the apical pyridine ligand is not involved in the SOMOs. Therefore, the $\mathbf{6_S}$→$\mathbf{6_T}$ intersystem crossing is less facile, as quantitatively supported by calculations. In the case of the carbonylated complex, the minimum-energy crossing point (MECP)[47] was found to be null.[27] Conversely, an appropriate scan for the $\mathbf{6_S}$→$\mathbf{6_T}$ interconversion (see Figure S3) shows that $\mathbf{6_S}$ lies constantly below $\mathbf{6_T}$, except for very short Ru–N_{py} distances (< 2.02 Å), for which the isomers become isoenergetic. Distinct MECP values of +3.8 and +6.6 kcal mol^{-1} were determined for $\mathbf{6_S}$ and $\mathbf{6_T}$, respectively, confirming a more hindered spin crossing. This is also consistent with the computed spin-density distribution in $\mathbf{6_T}$ (Figure S4), which shows smaller spin accumulation at the N imido atom compared to $\mathbf{C_T}$ (0.9 vs. 1.59 e^2 bohr^{-3}). The trend is opposite at the ruthenium centre (0.72 vs. 0.31 e^2 bohr^{-3}).

The subtle but evident electronic differences do not seem to preclude a radical pathway, which starts with $\mathbf{6_T}$ (Scheme 5) and can be related to the profile of Scheme 3. Otherwise, the singlet $\mathbf{6_S}$ may lose its pyridine ligand to afford the intermediate [Ru](NR) (**12**) at the relatively small energy cost of +7.4 kcal mol^{-1}. As discussed below, the catalysis may still proceed from **12** with a different pattern.

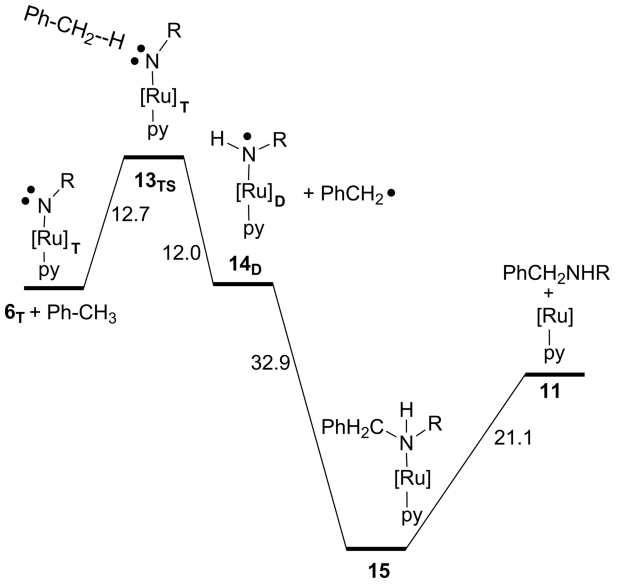

Scheme 5. Energy profile for formation of the benzylic amine $PhCH_2NHR$ starting from $\mathbf{6_T}$.

As occurs at $\mathbf{C_T}$, the radical activation of the organic substrate is already enhanced at the TS $\mathbf{13_{TS}}$ (Figure 4). The corresponding barrier appears somewhat higher than that of $\mathbf{8_{TS}}$ for the process promoted by **1** in Scheme 3 (+12.7 vs. +9.1 kcal mol^{-1}), but in both cases one methylic H atom of toluene already lies halfway between the methylic carbon atom and the N acceptor, given that the C–H and N–H distances in $\mathbf{13_{TS}}$ are 1.34 and 1.28 Å, respectively. At this point, the spin densities at the Ru and N_{imido} atoms are 0.36, 0.98 e^2 bohr^{-3}, respectively, and the exocyclic carbon atom of the tolyl ring has also large spin localisation (0.60 e^2 bohr^{-3}).

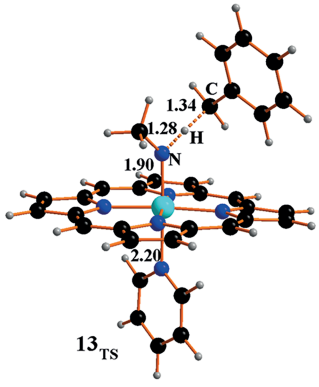

Figure 4. Optimised structure of {[Ru](py)$(NR)_T$*$(PhCH_3)_{TS}$} ($\mathbf{13_{TS}}$).

In the next step, the radical $PhCH_2^{\bullet}$ is fully separated from the doublet [Ru](py)$(NHR)_D$ ($\mathbf{14_D}$ in Figure 5, a) with an energy gain close to that of the corresponding separation from $\mathbf{9_D}$ in Scheme 3 (–13.0 vs. –12.0 kcal mol^{-1}). In $\mathbf{14_D}$ the radical character at the amidic N atom (0.61 e^2 bohr^{-3}) is almost twice that of the ruthenium atom, which suggests a new prompt coupling with $PhCH_2^{\bullet}$ to yield the diamagnetic product [Ru](py){$HN(R)CH_2Ph$}$_S$ (**15**) of Figure 5 (b). The energy balance is exergonic by –32.9 kcal mol^{-1}.

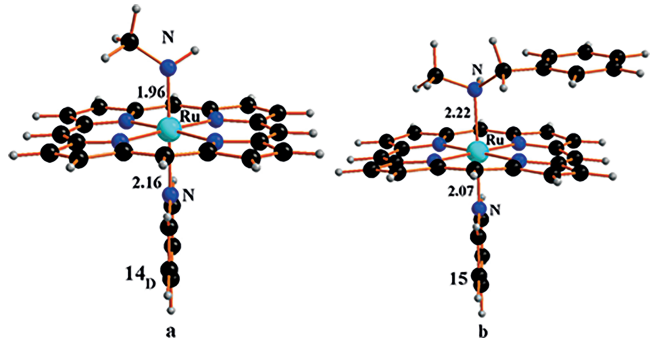

Figure 5. Optimised structure of: a) ([Ru](py)$(NHR)_D$ ($\mathbf{14_D}$) and b) [Ru](py){$HN(R)CH_2Ph$} (**15**).

Finally, the separation of the benzylic amine $PhCH_2NHR$ from **15** is endergonic by +21.1 kcal mol^{-1}, an energy cost similar to that calculated for removing one pyridine ligand from the starting complex [Ru](py)$_2$ (**2**). The departure of the benzylic amine restores the catalyst [Ru](py) (**11**), which is available for a new catalytic cycle. Concerning the overall free-energy balance of the process, the benzylic amination described in Equation (1) catalysed by the pyridine complex **11** is more exergonic than that promoted by the corresponding [Ru](CO) (**1**) catalyst (–43.3 vs. –37.2 kcal mol^{-1}, respectively). However, whereas **1** is directly available for azide activation, **11** must be first generated from the bis-pyridine precursor **2**, which has a high energy cost of +22.1 kcal mol^{-1}.

$$RN_3 + PhCH_3 \rightarrow PhCH_2NHR + N_2 \quad (1)$$

Benzylic Amination Catalysed by [Ru](NR)$_2$

Cycle (a) of Scheme 2 for the allylic amination promoted by catalyst **1** is not the only possible process. In particular, the bis-imido species [Ru](NR)$_2$ ($\mathbf{E_S}$) can independently behave as a catalyst for the comparable amination process shown in cycle (b) of Scheme 2.[27] Species $\mathbf{E_S}$ is obtained as a side product of cycle (a) when the mono-imido complex $\mathbf{C_S}$ is not promptly transformed into the triplet isomer $\mathbf{C_T}$. In fact, the singlet $\mathbf{C_S}$ has a chance of losing the weakly bound CO ligand to form the five-coordinate complex [Ru](NR), which allows access to cycle (b). Although no mono-imido species of the type $\mathbf{C_S}$ or $\mathbf{C_T}$ has been ever isolated, their computational study accounts for a series of experimental facts. Another azide molecule can be anchored and activated at the vacant site of [Ru](NR), similar to what happens at complex **1**. The subsequent N_2 loss gen-

erates the bis-imido singlet [Ru](NR)$_2$ ($\mathbf{E_S}$), which can be converted to the triplet isomer $\mathbf{E_T}$. Such an intersystem crossing is significantly endergonic, at variance with the $\mathbf{C_S}$→$\mathbf{C_T}$ process, but the cost of +16.1 kcal mol^{-1} may not be an insurmountable barrier in view of the high working temperatures. In $\mathbf{E_T}$,[27] the two unpaired spins are initially shared by the two NR groups, but the C–H bond activation still occurs only at one of them (Scheme 2) to provide the doublet [Ru](NR)(NHR)$_D$, in which the surviving unpaired electron is largely localised at the amido ligand. The subsequent spin pairing of the amido complex with the previously separated allylic radical $C_6H_9^{\cdot}$ is again consistent with the rebound mechanism affording the allyl amine (C_6H_9)NHR. The overall process is exergonic by –40.6 kcal mol^{-1}.

Our present experimental and computational studies on the catalytic activity of **2** in the benzylic amination of toluene also support the alternative formation of the diamagnetic bis-imido complex [Ru](NR)$_2$ ($\mathbf{E_S}$), from which a cycle of type (b) may be initiated. Scheme 4 shows the energy profile for the transformation of **2** into the five-coordinate singlet [Ru](NR) (**12**), which provides access to cycle (b) of Scheme 2, which was already described for the allylic amination.[27]

To obtain a comparable quantitative overview for the benzylic amination of PhCH$_3$, corresponding DFT calculations were carried out starting from triplet isomer [Ru](NR)$_2$ ($\mathbf{E_T}$). It was found that the initial adduct [$\mathbf{E_T}$*PhCH$_3$]$_{TS}$ ($\mathbf{16_{TS}}$) (Figure 6) is again a key TS with a ΔG barrier of +10.4 kcal mol^{-1}, which is smaller than that for the amination of cyclohexene (+14.0 kcal mol^{-1}).[48] On the other hand, some evident energy differences emerge after $\mathbf{16_{TS}}$: (1) the separation of the organic radical ($PhCH_2^{\cdot}$ or $C_6H_9^{\cdot}$) from the amido imido doublet [Ru](NR)(NHR)$_D$ is exergonic by –16.4 and –26.8 kcal mol^{-1} for toluene and cyclohexene, respectively; (2) the rebound mechanism to form the complex [Ru](NR){HN(R)CH$_2$Ph} (**17**) (Figure 7) is more exergonic than in the case of cyclohexene amination (–36.0 vs. –27.8 kcal mol^{-1}); (3) the energy cost to release the amine product is approximately halved for benzylamine (+10.5 vs. +21.1 kcal mol^{-1}).

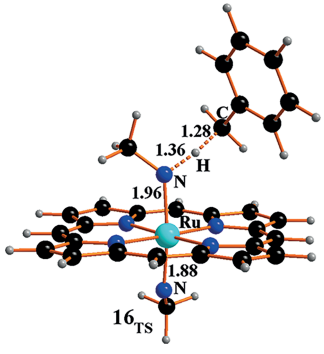

Figure 6. Optimised structure of [$\mathbf{E_T}$*PhCH$_3$]$_{TS}$ ($\mathbf{16_{TS}}$).

The somewhat contrasting trends do not clearly allow one to establish which amination process (allylic vs. benzylic) is more efficient. Conversely, the most important conclusion is that the catalytic process, initiated by **1** or **2**, eventually becomes a unique type that involves the same bis-imido species [Ru](NR)$_2$. ($\mathbf{E_S}$).

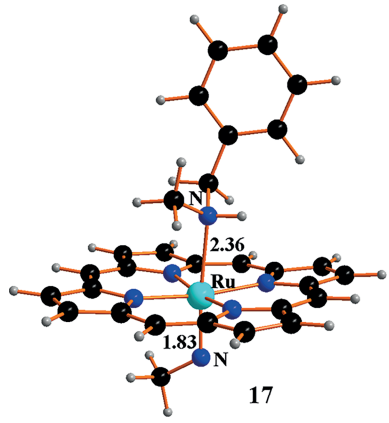

Figure 7. Optimised structure of [Ru](NR){HN(R)CH$_2$Ph} (**17**).

Conclusions

The present work has illustrated the experimental catalytic activity of Ru(TPP)(py)$_2$ (**2**) in promoting the amination of benzylic C–H bonds by aryl azides. Complex **2** showed comparable behaviour to the already studied Ru(TPP)(CO) (**1**), which suggests that the dependence of the catalytic activity on the nature of different axial ligands is of secondary importance. Experimental results were corroborated by DFT analyses, which contributed to rationalising key aspects of the catalytic mechanism, also by elaborating a previously developed model of the **1**-catalysed allylic amination of cyclohexene.

The loss of one pyridine ligand from the precatalyst **2** affords the active catalyst [Ru](py) (**11**) with a rather endergonic balance, which seems to disfavour the catalytic process, at least in the beginning. On the other hand, this step is essential to allow coordination of the azide reactant to the metal centre and its subsequent activation with eco-friendly release of N_2. It was found that this process occurs through a TS with common features in all the studied cases. The subsequent mono-imido complexes {e.g., [Ru](py)(NR) ($\mathbf{6_S}$) or [Ru](CO)(NR) ($\mathbf{C_S}$)} transform, more or less easily, into their triplet isomers ($\mathbf{6_T}$ or $\mathbf{C_T}$), which essentially promote the radical activation of a C–H bond of the studied benzylic substrate. Two subsequent spin couplings allow the formation of the benzylic amine product, according to the known rebound mechanism.[34] Alternatively, the mono-imido singlet $\mathbf{C_S}$ or $\mathbf{6_S}$ may lose the apical ligand *trans* to the NR ligand, which is CO or pyridine. The vacated coordination site allows another azide activation, which in any case leads to the same bis-imido complex [Ru](NR)$_2$. This complex may also exist as a singlet ($\mathbf{E_S}$) or a triplet ($\mathbf{E_T}$), but only the latter supports the radical activation of the benzylic substrate and affords benzylic amine through the known rebound mechanism. Importantly, the process cata-

lysed by $\mathbf{E_S}$ and $\mathbf{E_T}$ does not depend on whether the bis-imido catalyst was generated from precursor **1** or **2**.

Experimental Section

General Conditions: All reactions were performed in a nitrogen atmosphere by employing standard Schlenk techniques and vacuum-line manipulations. Benzene, toluene, cyclohexene, cumene, pyridine and dichloromethane were purified by distillation under nitrogen in the presence of CaH_2 or Na. All the other starting materials were commercial products used after degasification.

Solvents and Reagents: 3,5-Bis(trifluoromethyl)phenyl azide,[49] 4-*tert*-butylphenyl azide,[50] $TPPH_2$,[51] Ru(TPP)(CO) (**1**),[52] Ru(TPP)(CO)(MeOH),[36] Ru(TPP)(py)$_2$ (**2**),[41] Ru(TPP)(NAr)$_2$ (**7**) {Ar = 3,5-bis(trifluoromethyl)phenyl}[18] and methyl hydrocinnamate[53] were synthesised by methods reported in the literature or using minor modifications thereof.

Instruments: NMR spectra were recorded at 300 K (unless otherwise specified) and 300 or 400 MHz for ^{1}H. IR, UV/Vis and mass spectra were recorded in the analytical laboratories of Milan University.

Computational Details: All calculations were carried out with the Gaussian 09 package[54] at the B97D-DFT[46] level of theory. The TPP ligand ($C_{44}H_{28}N_4$) was replaced by porphine ($C_{20}H_{14}N_4$), which has H atoms in place of Ph groups at the *meso* positions, in all DFT calculations. In addition, the simple CH_3N_3 was used in place of the experimentally used 3,5-bis(trifluoromethyl)phenyl azide reactant. All optimised structures were validated as minima and/or transition states by calculation of vibrational frequencies. The transition states along the reaction pathways were also validated through Intrinsic Reaction Coordinate (IRC) calculations.[55] All calculations were based on the CPCM[56] model for the benzene solvent, the same as used in the experiments. The effective Stuttgart/Dresden core potential (SDD)[57] was adopted for the ruthenium centre, while for all the other atomic species the basis set was 6-31G, with addition of the polarisation functions (d,p). The coordinates of all the optimised structures are reported in the Supporting Information.

Synthesis of Ru(TPP)(dmso)$_2$ (4):[58] Ru(TPP)(py)$_2$ (13.7 mg, 1.54×10^{-2} mmol) was suspended in DMSO (2.0 mL), and the resulting solution was heated at 110 °C for 4.0 h. The solution was evaporated to dryness and the crystalline violet solid was dried in vacuo. Analytical data were in accord with those reported in the literature.

General Procedures for Catalytic Reactions: In a typical run, the aryl azide and the ruthenium catalyst (6.0 mg, 6.8×10^{-3} mmol) were dissolved in the hydrocarbon (15 mL). The resulting mixture was heated in a preheated oil bath until complete consumption of the azide. The catalytic reaction was monitored by IR spectroscopy by measuring the characteristic N_3 absorbance at about 2115 cm^{-1}. The reaction was considered finished when the absorbance value of the azide was less than 0.01 (by using a 0.1 mm-thick cell). The solvent was evaporated to dryness and the residue analysed by ^{1}H NMR analysis with 2,4-dinitrotoluene as the internal standard.

Analytical data of **3a**,[19] **3b**,[19] **3c**,[59] **3d**,[19] **3e**,[19] **3f**,[19] **3g**,[33] **3h**[33] and **3i**[60] were in accord with those reported in the literature.

Acknowledgments

C. M. and G. M. acknowledge the Italian SuperComputing Research Allocation-Consorzio Interuniversitario per la gestione del centro di calcolo elettronico dell'Italia Nord-Orientale (ISCRA-CINECA) (HP grant "HP10BEG2NO") and the Centro Ricerche Energia e Ambiente (CREA), Colle Val d'Elsa, Siena, Italy, for computational resources.

[1] E. Dux, *Chem. Rev. (Deddington, U. K.)* **2009**, *19*, 11–15.
[2] J. C. Lewis, R. G. Bergman, J. A. Ellman, *Acc. Chem. Res.* **2008**, *41*, 1013–1025.
[3] *Organic Azides: Syntheses and Applications* (Eds.: S. Bräse, K. Banert), Wiley, Chichester, UK, **2010**.
[4] S. Bräse, C. Gil, K. Knepper, V. Zimmermann, *Angew. Chem. Int. Ed.* **2005**, *44*, 5188–5240; *Angew. Chem.* **2005**, *117*, 5320.
[5] S. Cenini, E. Gallo, A. Caselli, F. Ragaini, S. Fantauzzi, C. Piangiolino, *Coord. Chem. Rev.* **2006**, *250*, 1234–1253.
[6] S. Cenini, F. Ragaini, E. Gallo, A. Caselli, *Curr. Org. Chem.* **2011**, *15*, 1578–1592.
[7] S. Chiba, *Synlett* **2012**, *23*, 21–44.
[8] T. G. Driver, *Org. Biomol. Chem.* **2010**, *8*, 3831–3846.
[9] T. Katsuki, *Chem. Lett.* **2005**, *34*, 1304–1309.
[10] M. Minozzi, D. Nanni, P. Spagnolo, *Chem. Eur. J.* **2009**, *15*, 7830–7840.
[11] M. Y. Weber, G. Yilmaz, G. Wille, *Chim. Oggi-Chem. Today* **2011**, *29*, 8–10.
[12] S. Cenini, E. Gallo, A. Penoni, F. Ragaini, S. Tollari, *Chem. Commun.* **2000**, 2265–2266.
[13] S. Fantauzzi, A. Caselli, E. Gallo, *Dalton Trans.* **2009**, 5434–5443.
[14] F. Ragaini, A. Penoni, E. Gallo, S. Tollari, C. L. Gotti, M. Lapadula, E. Mangioni, S. Cenini, *Chem. Eur. J.* **2003**, *9*, 249–259.
[15] A. Caselli, E. Gallo, S. Fantauzzi, S. Morlacchi, F. Ragaini, S. Cenini, *Eur. J. Inorg. Chem.* **2008**, 3009–3019.
[16] T. W.-S. Chow, G.-Q. Chen, Y. Liu, C.-Y. Zhou, C.-M. Che, *Pure Appl. Chem.* **2012**, *84*, 1685–1704.
[17] S. Fantauzzi, E. Gallo, A. Caselli, C. Piangiolino, F. Ragaini, S. Cenini, *Eur. J. Org. Chem.* **2007**, 6053–6059.
[18] S. Fantauzzi, E. Gallo, A. Caselli, F. Ragaini, N. Casati, P. Macchi, S. Cenini, *Chem. Commun.* **2009**, 3952–3954.
[19] D. Intrieri, A. Caselli, F. Ragaini, S. Cenini, E. Gallo, *J. Porphyrins Phthalocyanines* **2010**, *14*, 732–740.
[20] D. Intrieri, A. Caselli, F. Ragaini, P. Macchi, N. Casati, E. Gallo, *Eur. J. Inorg. Chem.* **2012**, 569–580.
[21] D. Intrieri, M. Mariani, A. Caselli, F. Ragaini, E. Gallo, *Chem. Eur. J.* **2012**, *18*, 10487–10490.
[22] Y. Liu, C.-M. Che, *Chem. Eur. J.* **2010**, *16*, 10494–10501.
[23] H.-J. Lu, V. Subbarayan, J.-R. Tao, X. P. Zhang, *Organometallics* **2010**, *29*, 389–393.
[24] H. Lu, H. Jiang, L. Wojtas, X. P. Zhang, *Angew. Chem. Int. Ed.* **2010**, *49*, 10192–10196; *Angew. Chem.* **2010**, *122*, 10390.
[25] H. Lu, J. Tao, J. E. Jones, L. Wojtas, X. P. Zhang, *Org. Lett.* **2010**, *12*, 1248–1251.
[26] H. Lu, X. P. Zhang, *Chem. Soc. Rev.* **2011**, *40*, 1899–1909.
[27] a) G. Manca, E. Gallo, D. Intrieri, C. Mealli, *ACS Catal.* **2014**, *4*, 823–832; b) P. Zardi, A. Pozzoli, F. Ferretti, G. Manca, C. Mealli, E. Gallo, *Dalton Trans.* **2015**, *44*, 10479–10489.
[28] C. Piangiolino, E. Gallo, A. Caselli, S. Fantauzzi, F. Ragaini, S. Cenini, *Eur. J. Org. Chem.* **2007**, 743–750.
[29] P. Zardi, D. Intrieri, A. Caselli, E. Gallo, *J. Organomet. Chem.* **2012**, *716*, 269–274.
[30] C.-M. Che, V. K.-Y. Lo, C.-Y. Zhou, J.-S. Huang, *Chem. Soc. Rev.* **2011**, *40*, 1950–1975.
[31] A. Caselli, E. Gallo, F. Ragaini, F. Ricatto, G. Abbiati, S. Cenini, *Inorg. Chim. Acta* **2006**, *359*, 2924–2932.
[32] H. Lu, Y. Hu, H. Jiang, L. Wojtas, X. P. Zhang, *Org. Lett.* **2012**, *14*, 5158–5161.
[33] P. Zardi, A. Caselli, P. Macchi, F. Ferretti, E. Gallo, *Organometallics* **2014**, *33*, 2210–2218.
[34] J. T. Groves, *J. Chem. Educ.* **1985**, *62*, 928–931.
[35] G. M. Brown, F. R. Hopf, J. A. Ferguson, T. J. Meyer, D. G. Whitten, *J. Am. Chem. Soc.* **1973**, *95*, 5939–5942.

[36] J. P. Collman, C. E. Barnes, P. N. Swepston, J. A. Ibers, *J. Am. Chem. Soc.* **1984**, *106*, 3500–3510.
[37] J. P. Collman, S. T. Harford, S. Franzen, J.-C. Marchon, P. Maldivi, A. P. Shreve, W. H. Woodruff, *Inorg. Chem.* **1999**, *38*, 2085–2092.
[38] S. C. Jeoung, D. Kim, D. W. Cho, M. Yoon, K.-H. Ahn, *J. Phys. Chem.* **1996**, *100*, 8867–8874.
[39] D. Kim, Y. O. Su, T. G. Spiro, *Inorg. Chem.* **1986**, *25*, 3993–3997.
[40] I. R. Paeng, K. Nakamoto, *J. Am. Chem. Soc.* **1990**, *112*, 3289–3297.
[41] S. E. Vitols, R. Kumble, M. E. Blackwood, J. S. Roman, T. G. Spiro, *J. Phys. Chem.* **1996**, *100*, 4180–4187.
[42] M. Barley, D. Dolphin, B. R. James, C. Kirmaier, D. Holten, *J. Am. Chem. Soc.* **1984**, *106*, 3937–3943.
[43] C. D. Tait, D. Holten, M. Barley, D. Dolphin, B. R. James, *J. Am. Chem. Soc.* **1985**, *107*, 1930–1934.
[44] a) J. P. Collman, J. I. Brauman, J. P. Fitzgerald, J. W. Sparapany, J. A. Ibers, *J. Am. Chem. Soc.* **1988**, *110*, 3486–3495; b) Y. Li, P. W. Hong Chan, N.-Y. Zhu, C.-M. Che, H.-L. Kwong, *Organometallics* **2004**, *23*, 54–66.
[45] a) F. R. Hopf, T. P. O'Brien, W. R. Scheidt, D. G. Whitten, *J. Am. Chem. Soc.* **1975**, *97*, 277–281; b) F. Malvolti, P. Le Maux, L. Toupet, M. E. Smith, W. Y. Man, P. J. Low, E. Galardon, G. Simmonneaux, F. Paul, *Inorg. Chem.* **2010**, *49*, 9101–9103.
[46] S. Grimme, *J. Comput. Chem.* **2006**, *27*, 1787–1799.
[47] a) J. N. Harvey, R. Poli, K. M. Smith, *Coord. Chem. Rev.* **2003**, *238–239*, 347–361; b) J. N. Harvey, M. Aschi, *J. Chem. Soc. Faraday Trans.* **2003**, *124*, 129–143.
[48] A very reliable comparison of the barriers is not possible, since for technical reasons, the energy of the cyclohexene TS was estimated only as ΔE (electronic energy). In these terms, the barrier is higher for cyclohexene than toluene (+3.0 vs. +0.2 kcal mol^{-1}), but the difference should remain also in terms of the free energy ΔG, under the assumption that the entropic component computed for toluene ($-T\Delta S$) is +10 kcal mol^{-1}.
[49] M. Tanno, S. Sueyoshi, S. Kamiya, *Chem. Pharm. Bull.* **1982**, *30*, 3125–3132.
[50] J. B. Gerken, M. L. Rigsby, R. E. Ruther, R. J. Pérez-Rodríguez, I. A. Guzei, R. J. Hamers, S. S. Stahl, *Inorg. Chem.* **2013**, *52*, 2796–2798.
[51] A. D. Adler, F. R. Longo, J. D. Finarelli, J. Goldmacher, J. Assour, L. Korsakoff, *J. Org. Chem.* **1967**, *32*, 476.
[52] J. P. Collman, A. O. Chong, G. B. Jameson, R. T. Oakley, E. Rose, E. R. Schmittou, J. A. Ibers, *J. Am. Chem. Soc.* **1981**, *103*, 516–533.
[53] A. W. Ingersoll, *Org. Synth.* **1929**, *9*, 42.
[54] M. J. Frisch, G. W. Trucks, H. B. Schlegel, G. E. Scuseria, M. A. Robb, J. R. Cheeseman, G. Scalmani, V. Barone, B. Mennucci, G. A. Petersson, H. Nakatsuji, M. Caricato, X. Li, H. P. Hratchian, A. F. Izmaylov, J. Bloino, G. Zheng, J. L. Sonnenberg, M. Hada, M. Ehara, K. Toyota, R. Fukuda, J. Hasegawa, M. Ishida, T. Nakajima, Y. Honda, O. Kitao, H. Nakai, T. Vreven, J. A. Montgomery Jr., J. E. Peralta, F. Ogliaro, M. Bearpark, J. J. Heyd, E. Brothers, K. N. Kudin, V. N. Staroverov, R. Kobayashi, J. Normand, K. Raghavachari, A. Rendell, J. C. Burant, S. S. Iyengar, J. Tomasi, M. Cossi, N. Rega, J. M. Millam, M. Klene, J. E. Knox, J. B. Cross, V. Bakken, C. Adamo, J. Jaramillo, R. Gomperts, R. E. Stratmann, O. Yazyev, A. J. Austin, R. Cammi, C. Pomelli, J. W. Ochterski, R. L. Martin, K. Morokuma, V. G. Zakrzewski, G. A. Voth, P. Salvador, J. J. Dannenberg, S. Dapprich, A. D. Daniels, Ö. Farkas, J. B. Foresman, J. V. Ortiz, J. Cioslowski, D. J. Fox, *Gaussian 09*, revision B.01, Gaussian, Inc., Wallingford CT, **2009**.
[55] K. Fukui, *Acc. Chem. Res.* **1981**, *14*, 363–368.
[56] a) V. Barone, M. Cossi, *J. Phys. Chem. A* **1998**, *102*, 1995–2001; b) M. Cossi, N. Rega, G. Scalmani, V. Barone, *J. Comput. Chem.* **2003**, *24*, 669–681.
[57] M. Dolg, H. Stoll, H. Preuss, R. M. Pitzer, *J. Phys. Chem.* **1993**, *97*, 5852–5859.
[58] E. Gallo, A. Caselli, F. Ragaini, S. Fantauzzi, N. Masciocchi, A. Sironi, S. Cenini, *Inorg. Chem.* **2005**, *44*, 2039–2049.
[59] S. Zhou, S. Fleischer, H. Jiao, K. Junge, M. Beller, *Adv. Synth. Catal.* **2014**, *356*, 3451–3455.
[60] F. Ragaini, S. Cenini, F. Turra, A. Caselli, *Tetrahedron* **2004**, *60*, 4989–4994.

Received: June 15, 2015
Published Online: September 18, 2015

